Chapter 12: Deformation and Deformation Tensors

THE STRAIN tensor, outlined in chapter eleven, is useful for calculating stretches of arbitrary lines and the components of shear and normal strain in a plane. However, the strain tensor does not include any information on the rotation history of a deformed volume, because it describes the strain ellipsoid shape only as determined by the axial ratios. A related tensor, which includes both the strain and rotation components of deformation, is the *deformation tensor*, *F*. The deformation tensor is useful, also, because knowledge of the tensor elements, F_{ij}, is sufficient to derive geologically important parameters, such as the stretches and orientation of the axes of the finite strain ellipse. The deformation tensor is introduced in this chapter.

Contents: The important distinction between coaxial and non-coaxial deformation is explained in section 12-1. Measures for 3D strain and shape parameters for the strain ellipsoid are outlined in section 12-2. Progressive deformation by pure shear and simple shear are highlighted in sections 12-3 and 12-4, respectively. The components of homogeneous deformation are distinguished in section 12-5. The deformation tensor is introduced in section 12-6. It is applied to calculate the change in length of principal stretches in section 12-7. The decomposition of the deformation tensor into its symmetric and skew-symmetric parts, valid only for infinitesimal deformations, is shown in section 12-8.

Practical hint: **Some relief from the laboratory sessions could be provided by organizing a field trip to natural outcrops with exemplary deformation patterns. A keen observer can find such exemplary features in almost any rock exposure.**

12-1 Coaxial and non-coaxial deformation

The deformation history of a rock body is determined by a continuous sequence of configurations through which the rock passes from the initial to the deformed state during progressive deformation. The deformation can be portrayed by either a deforming box or a deforming sphere, both arbitrary, but popular for their simple initial shapes. A major distinction must be made between homogeneous progressive deformations involving distortional rotation and those that do not. These are coaxial and non-coaxial deformations, respectively. During *coaxial deformations*, the strain ellipsoid remains stationary and involves no distortional rotation (Fig. 12-1a). The axes of the ellipsoid remain parallel (for each strain increment) at all times during the deformation. Likewise, any physical boundaries of a rock cube, parallel to the principal stress axes, will remain parallel to them, even after large strains.

Non-coaxial deformation involves distortional rotation, and the rotation angle, θ, of the strain ellipsoid, with respect to the non-rotating base of the marker cube, is an indirect measure of distortional rotation (Fig. 12-1b). A 3D deformation, where the strain ellipsoid is rotating about one of its principal axes of finite strain, is the most simple rotational strain possible. Geoscience literature has placed much emphasis on developing methods for practical strain measurement. It is emphasized here that strain, albeit an important component of distortion, is an incomplete measure of distortion if distortional rotation is involved. Distortion may include both strain and distortional rotation, which needs to be taken into account for a complete description of the deformation.

Coaxial deformations can be represented by the progressive distortion of either a normalized strain sphere into an ellipsoid or a unit cube into a rectangular body, all without any finite rotation of the strain axes. Figures 12-2a to d illustrate the

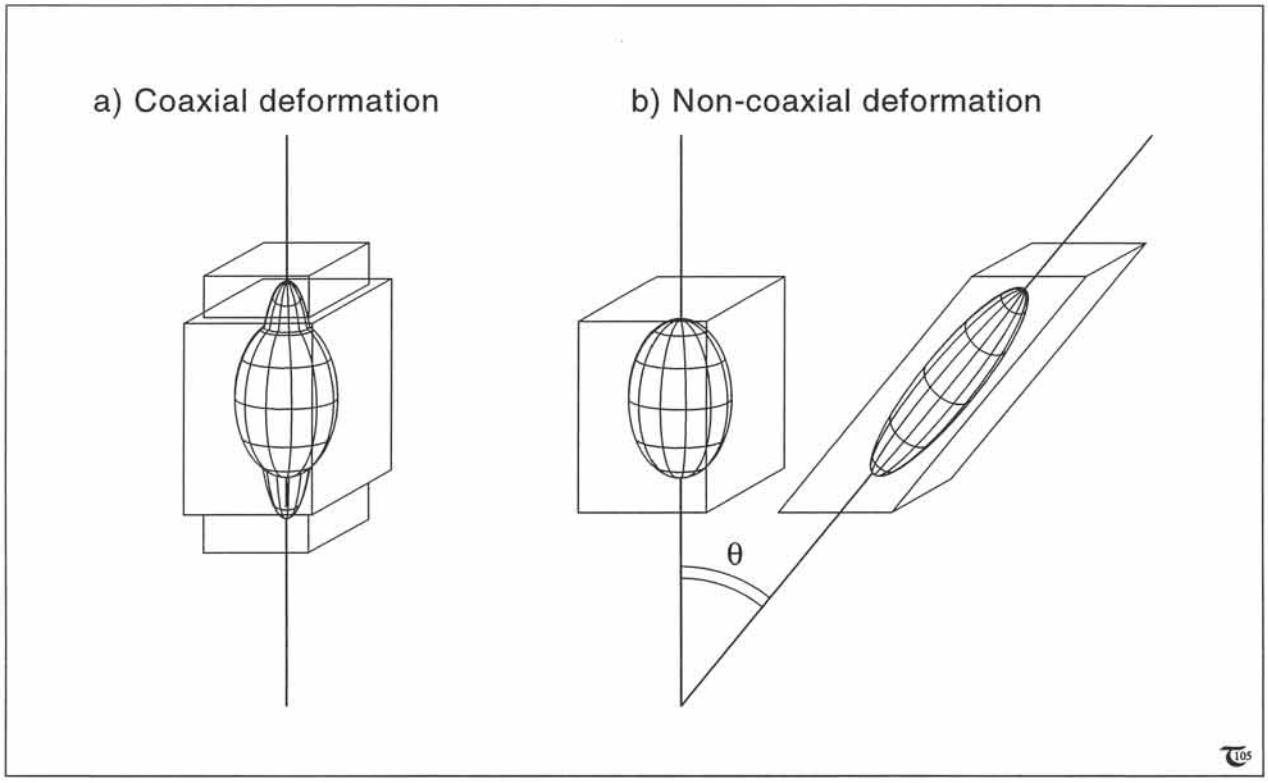

Figure 12-1: *a) & b) Coaxial and non-coaxial deformations.*

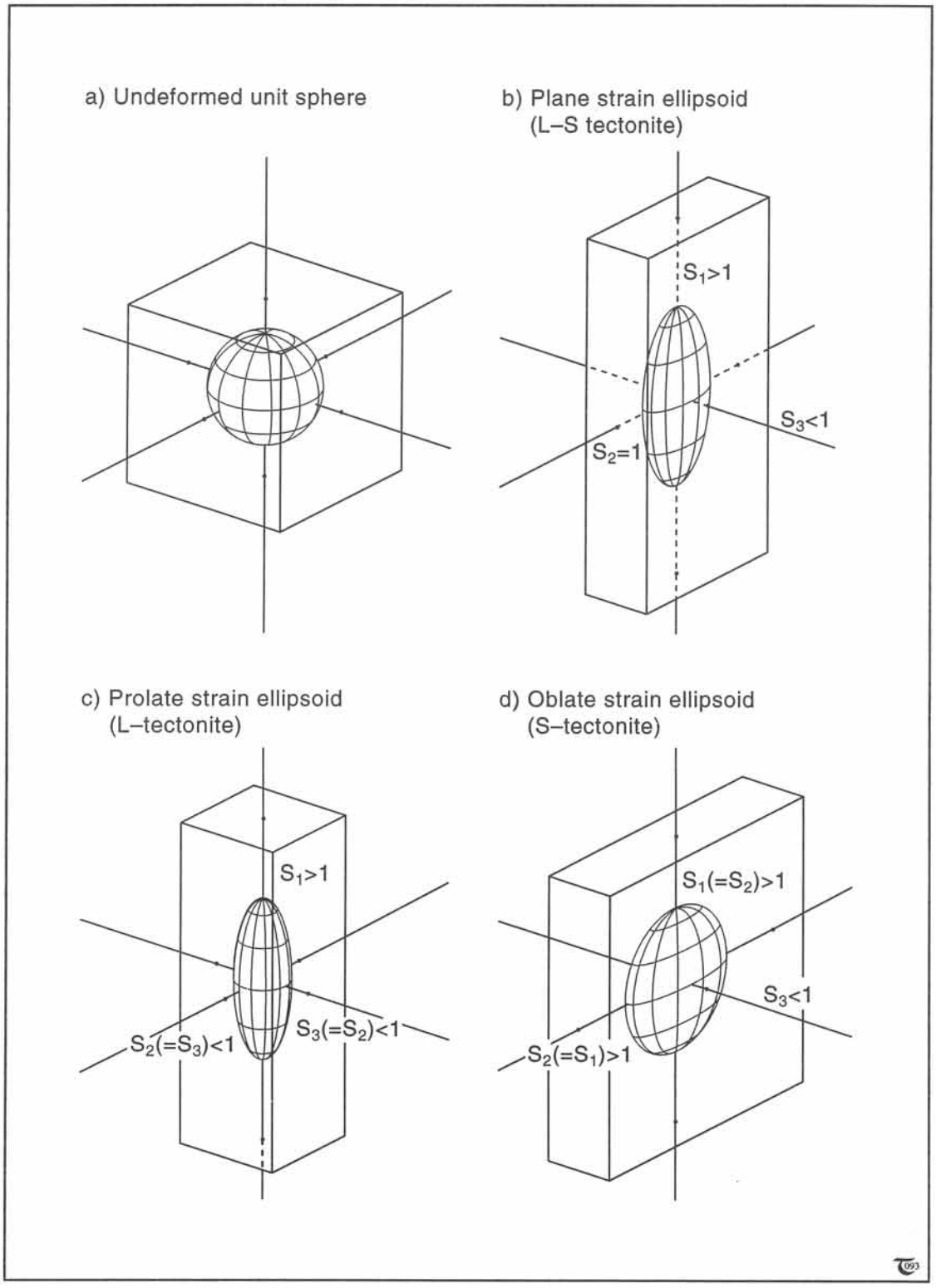

Figure 12-2: *a) to d) Undeformed unit sphere and three main types of ellipsoids, distinguished to classify finite strains in 3D deformations.*

distortion of a unit sphere inside a unit cube into plane strain, prolate, and oblate ellipsoids. The shape of a strain ellipsoid may vary between *prolate* ("cigar," Fig. 12-2c) and *oblate* ("pancake," Fig. 12-2d), and the corresponding rectangulars vary between square prisms and square tablets. The shape intermediate between prolate and oblate is represented by so-called *plane strain ellipsoids*, having one axis which retains unit length (Fig. 12-2b). Consequently, the intermediate axes of such plane strain ellipsoids do not change length during the deformation, i.e., $S_2=1$. Plane strain is generally considered the simplest type of homogeneous deformation, as it allows the analysis of strain in two dimensions. Two classical types of plane strain, pure shear and simple shear, are discussed in sections 12-3 and 12-4, respectively.

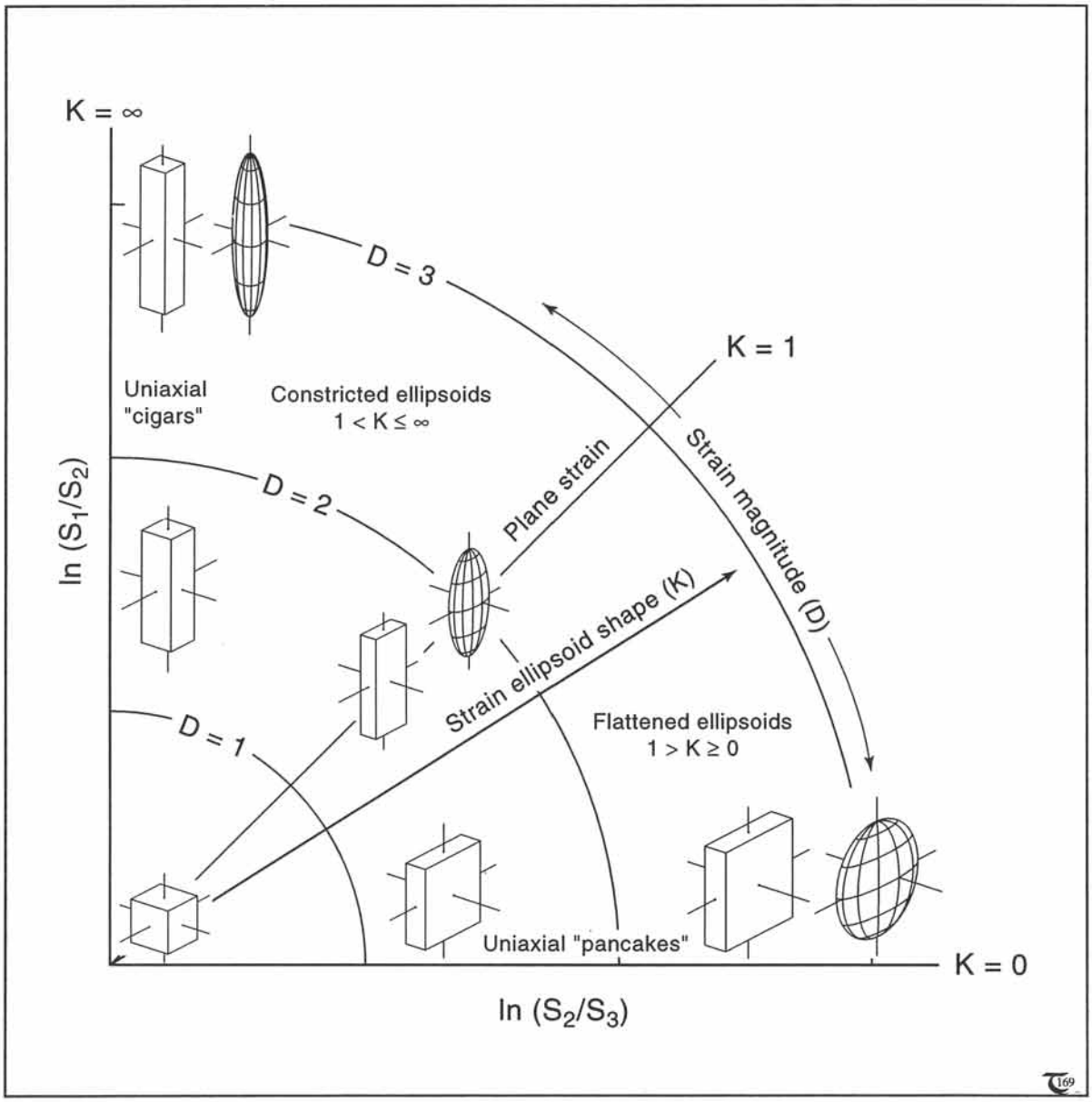

Figure 12-3: *Flinn plot. Each point in this plot represents a finite strain ellipsoid of a particular shape (K) and the magnitude of strain (D). Any rotational deformation is not accounted for.*

☐Exercise 12-1: Determine the type of strain for each of the following stretch values: (a) $S_1=2$, $S_2=1$, and $S_3=0.5$; (b) $S_1=4$, $S_2=0.5$, and $S_3=0.5$; and (c) $S_1=2$, $S_2=2$, and $S_3=0.25$. (d) Is there any volume change involved in the strains of a, b, or c?

☐Exercise 12-2: The principal planes of strain are mutually perpendicular and contain the principal stretch axes S_1, S_2, and S_3. To understand better the shape of 3D strain ellipsoids, draw cross-sections for each of the three principal planes for each of the following cases (using the data of exercise 12-1): a) plane strain, b) prolate strain, and c) oblate strain.

12-2 Measures for 3D strain and shape of ellipsoids

The shape of a finite strain ellipsoid in 3D is determined by the *relative* magnitude of the three principal stretches (S_1,S_2,S_3). The magnitude of the finite strain is determined by the *absolute* magnitude of the three principal stretches. However, it is of practical convenience to introduce an expression, generating a unique number for indicating the shape of a strain ellipsoid; likewise, a single measure of finite strain magnitude in 3D could sometimes be more practical than specifying all three principal stretches.

Many workers have suggested dimensionless *shape parameters* for classifying the strain ellipsoid shapes, using (S_1,S_2,S_3) in various alternative ways. Two of the most currently used shape factors are given here. Derek Flinn adapted, in 1962, earlier 1935 work by Zingg and introduced the k-value:

$$k=[(S_1/S_2)-1]/[(S_2/S_3)-1] \qquad (12\text{-}1a)$$

This measure was subsequently modified by, among others, John Ramsay, to use logarithmic strains and termed the *K-value*:

$$K=\ln(S_1/S_2)/\ln(S_2/S_3) \qquad (12\text{-}1b)$$

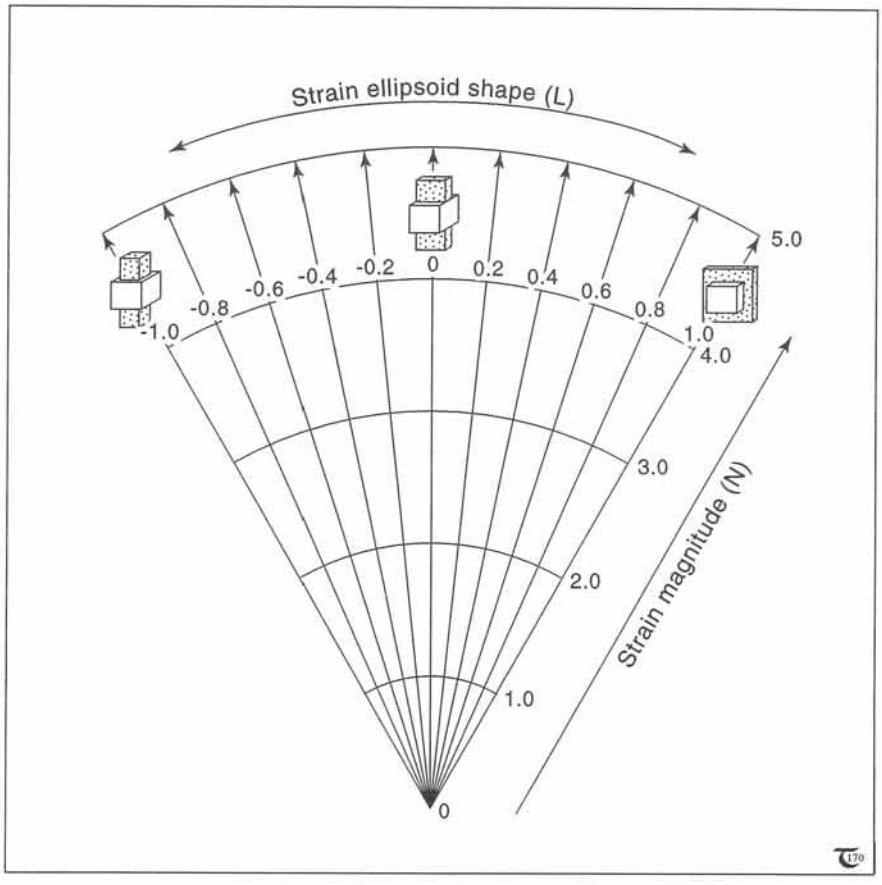

Figure 12-4: *Hsu plot. This is an alternative for the Flinn plot. The shape (L) and magnitude (N) parameters of a strain ellipsoid can be plotted as points in this diagram.*

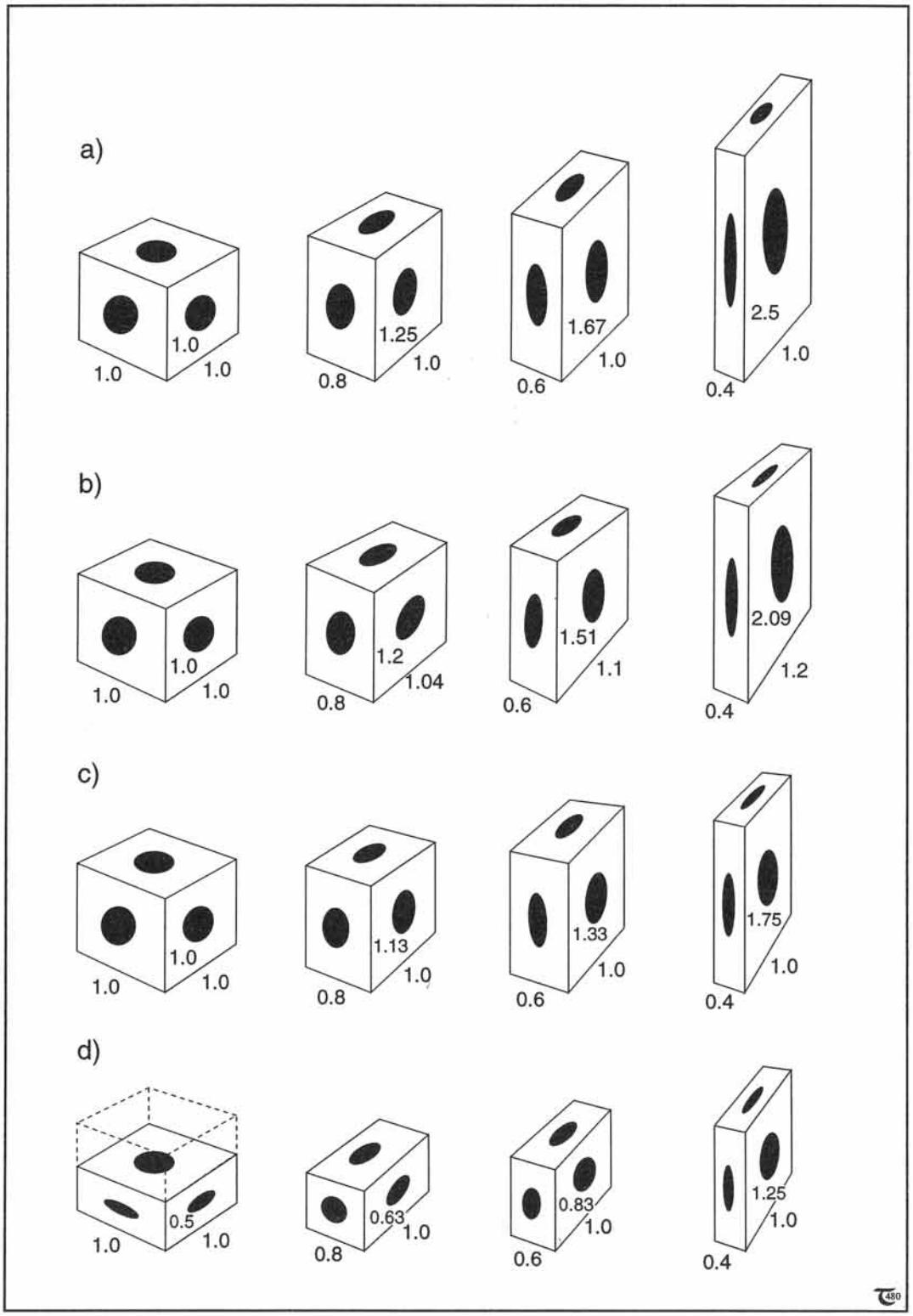

Figure 12-5: *a) to d) Four sequences of progressive deformation. Strain parameters are given in Table 12-1. See exercise 12-3.*

☐Exercise 12-3: Figure 12-5 shows four sequences of progressive deformation, all starting from a cube and deforming coaxially into rectangular blocks. Table 12-1 presents the three principal stretches for each block, including stretch ratios and their logarithms. a) Determine for each sequence what type of deformation is involved, i.e., plane strain, apparent constriction, true flattening, progressive volume loss, etc. b) Plot the shape of the ellipsoids and their strain magnitude for each of the the four sequences on a Flinn diagram. c) Also, plot the strain magnitude and shape on a Hsu plot.

The K- and k-values both yield unique numbers for unique shapes: unity for plane strain, infinity for ideal prolate strain ellipsoids, and zero for ideal oblate ellipsoids. Figure 12-3 shows a modern version of the so-called *Flinn plot*, which graphs $\ln(S_2/S_3)$ versus $\ln(S_1/S_2)$ and shows the possible spread in ellipsoid shapes. The Flinn plot is particularly useful to show the evolution history of a strain ellipsoid shape during progressive deformation. However, it does not differentiate between coaxial and non-coaxial strain histories.

A measure for the magnitude of the 2D strain is given by the *Ramsay strain parameter*, D:

$$D=[\ln^2(S_1/S_2)+\ln^2(S_2/S_3)]^{1/2} \qquad (12\text{-}2)$$

Contours of equal strain magnitude plot as circles in the Flinn plot of Figure 12-3, according to the circle equation (12-2).

Several alternatives are available to express the shape and strain magnitude of strain ellipsoids; one frequently used shape factor is *Lode's shape parameter*, L:

$$L=[\ln(S_2/S_3)-\ln(S_1/S_2)]/[\ln(S_2/S_3)+\ln(S_1/S_2)] \qquad (12\text{-}3)$$

The Lode shape factor is zero for plane strain, -1 for ideal prolate strain, and +1 for oblate strain ellipsoids. An alternative expression for the strain magnitude is *Nadai's strain parameter*, N:

$$N=[[\ln^2(S_1/S_2)+\ln^2(S_2/S_3)+\ln^2(S_3/S_1)]/3]^{1/2} \qquad (12\text{-}4)$$

The *Hsu plot* combines the Lode shape parameter and the Nadai strain parameter in an alternative for the Flinn plot (Fig. 12-4). The Flinn plot and classical Hsu

Table 12-1: *Principal stretches, their ratios and natural logarithms for each of the four deformation sequences shown in Figure 12-5. See exercise 12-3.*

	S_1	S_2	S_3	S_1/S_2	S_2/S_3	$\ln(S_1/S_2)$	$\ln(S_2/S_3)$
Series (a)							
Stage 1	1.00	1.00	1.00	1.00	1.00	0	0
Stage 2	1.25	1.00	0.80	1.25	1.25	0.22	0.22
Stage 3	1.67	1.00	0.60	1.67	1.67	0.51	0.51
Stage 4	2.50	1.00	0.40	2.50	2.50	0.92	0.92
Series (b)							
Stage 1	1.00	1.00	1.00	1.00	1.00	0	0
Stage 2	1.20	1.04	0.80	1.15	1.30	0.14	0.26
Stage 3	1.51	1.10	0.60	1.37	1.83	0.32	0.60
Stage 4	2.09	1.20	0.40	1.74	3.00	0.55	1.10
Series (c)							
Stage 1	1.00	1.00	1.00	1.00	1.00	0	0
Stage 2	1.13	1.00	0.80	1.13	1.25	0.12	0.22
Stage 3	1.33	1.00	0.60	1.33	1.67	0.29	0.51
Stage 4	1.75	1.00	0.40	1.75	2.50	0.56	0.92
Series (d)							
Stage 1	0.50	1.00	1.00	1.00	2.00	0	0.69
Stage 2	0.63	1.00	0.80	1.25	1.26	0.22	0.23
Stage 3	0.83	1.00	0.60	1.20	1.38	0.18	0.32
Stage 4	1.25	1.00	0.40	1.25	2.50	0.22	0.92

plot have both been used in the geological literature. Neither of these plots differentiates between coaxial and non-coaxial strain histories.

12-3 Pure shear

It is common to distinguish between so-called rotational and non-rotational 2D deformations, whereby the strain ellipse either remains stationary or not. Non-rotational deformation in 2D is known as *pure shear deformation*, which develops plane strains only and involves no distortional rotation. Pure shear is simple to construct, because each of the new principal axes of the strain ellipse remains parallel to the original axes at all times during the deformation. Likewise, any physical boundaries of a rock cube, with ribs paralleling the principal strain (and stress) axes, remain parallel to them original axes even after large strains (Figs. 12-6a to e). The relative lengths of any deforming rectangle will be given by the principal stretches, S_1,S_2,S_3, with S_2 always retaining unity.

If strain is regarded as a series of superimposed small stretches, L_i, then the resulting total strain can be measured as a *logarithmic strain*, ϵ (also termed *natural strain* or *true strain*):

$$\epsilon=\sum(\delta L_i/L_0) \qquad (12\text{-}5a)$$

If δL_i is taken infinitesimally small:

$$\epsilon=\int(dL_i/L_0)= \ln(L/L_0)= \ln S \qquad (12\text{-}5b)$$

The change of the stretches S_1 and S_3 during progressive deformation has been graphed against the major natural strain, ϵ_1, in Figure 12-7, using equation (12-5b). The time, required for each increment of natural strain to accumulate, is constant for constant strain-rate deformations. This means that the horizontal axis of Figure 12-7 can alternatively be read as a non-dimensional time scale.

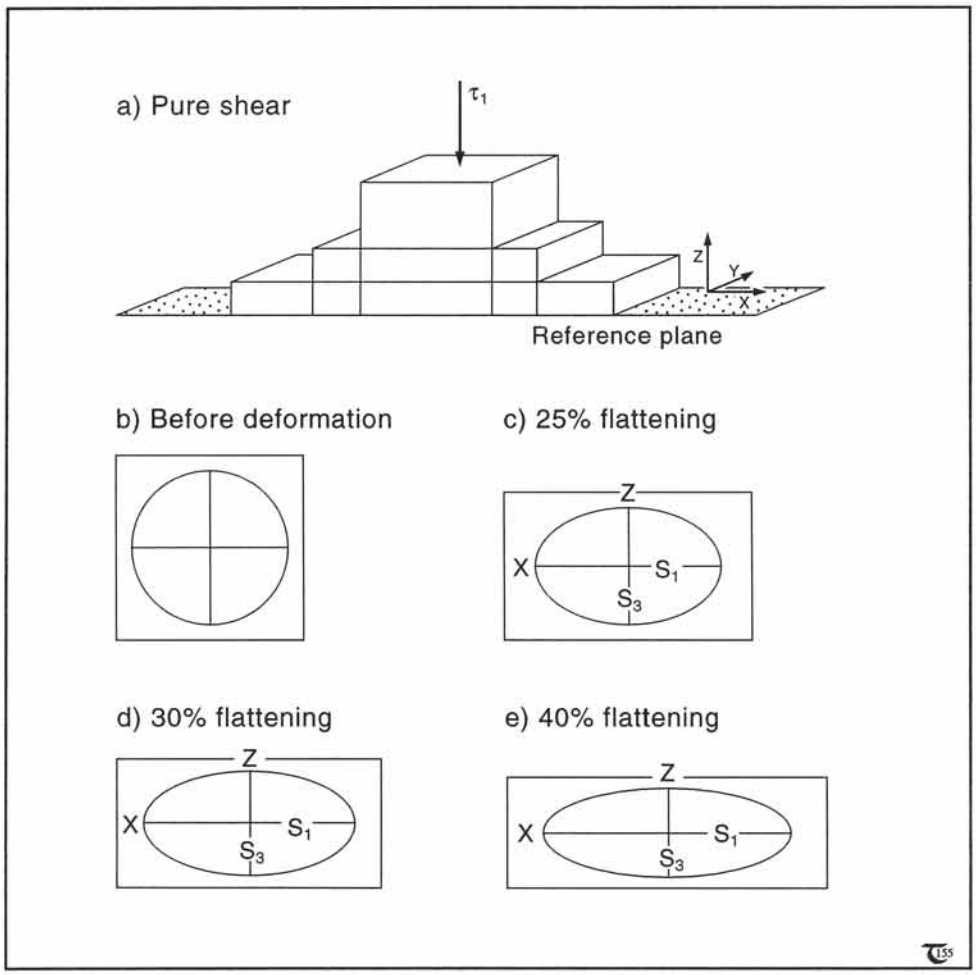

Figure 12-6: *a) to e) Principle sketch of pure shear deformation. The deformation is always by plane strain without rotation; this is a coaxial deformation.*

□Exercise 12-4: Examine the pure shears of Figure 12-6c to e. a) Plot the three major stretches, for each stage illustrated, against the natural strain, ϵ_1, in Figure 12-7. b) Also, plot the three minor stretches against the natural strain in the same diagram.

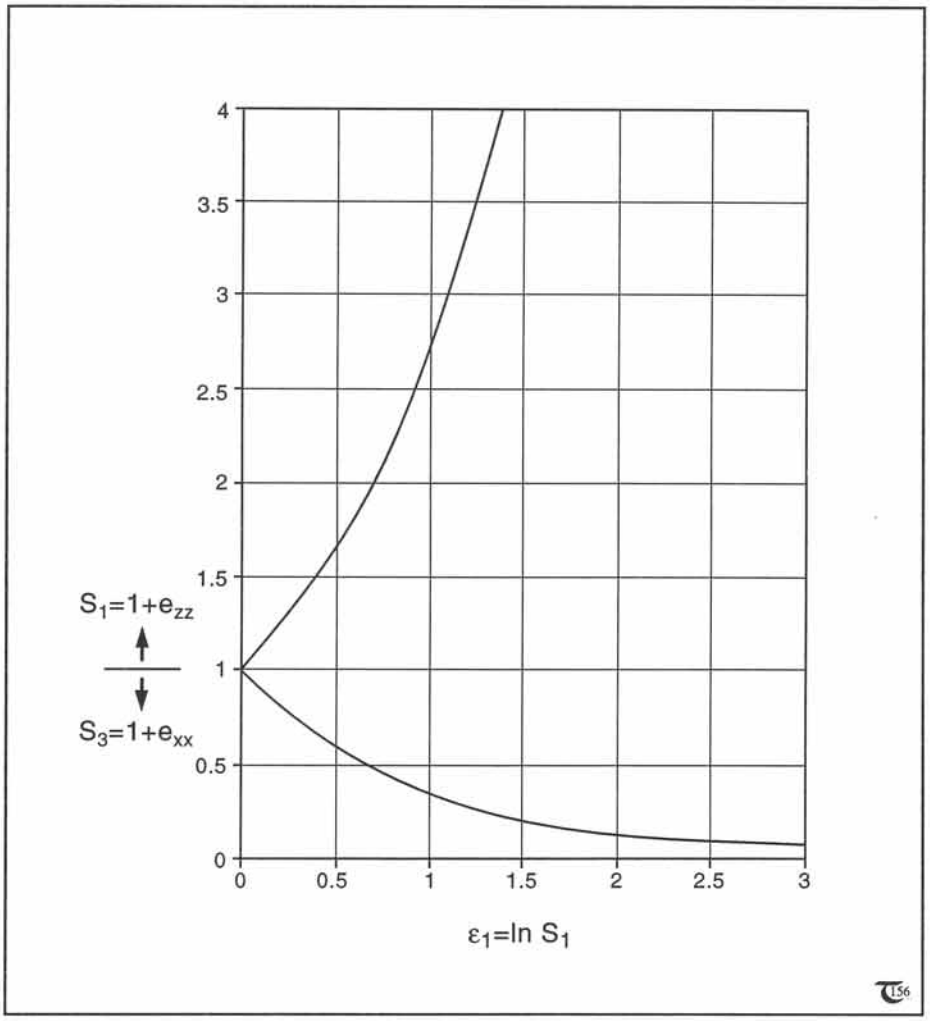

Figure 12-7: *Change of the principal stretches in pure shear deformation as a function of natural strain or non-dimensional time, if assuming constant strain-rate throughout.*

12-4 Simple shear

One particular type of *rotational deformation* in 2D, maintaining plane strain throughout, is known as *simple shear deformation*. Progressive simple shear is easy to construct, because it is a rotational deformation, where any of the lengths in the top and bottom planes of an initial cube remain constant throughout the deformation (Figs. 12-8a to e). The major principal stress for simple shear is consistently oriented at 45° to the

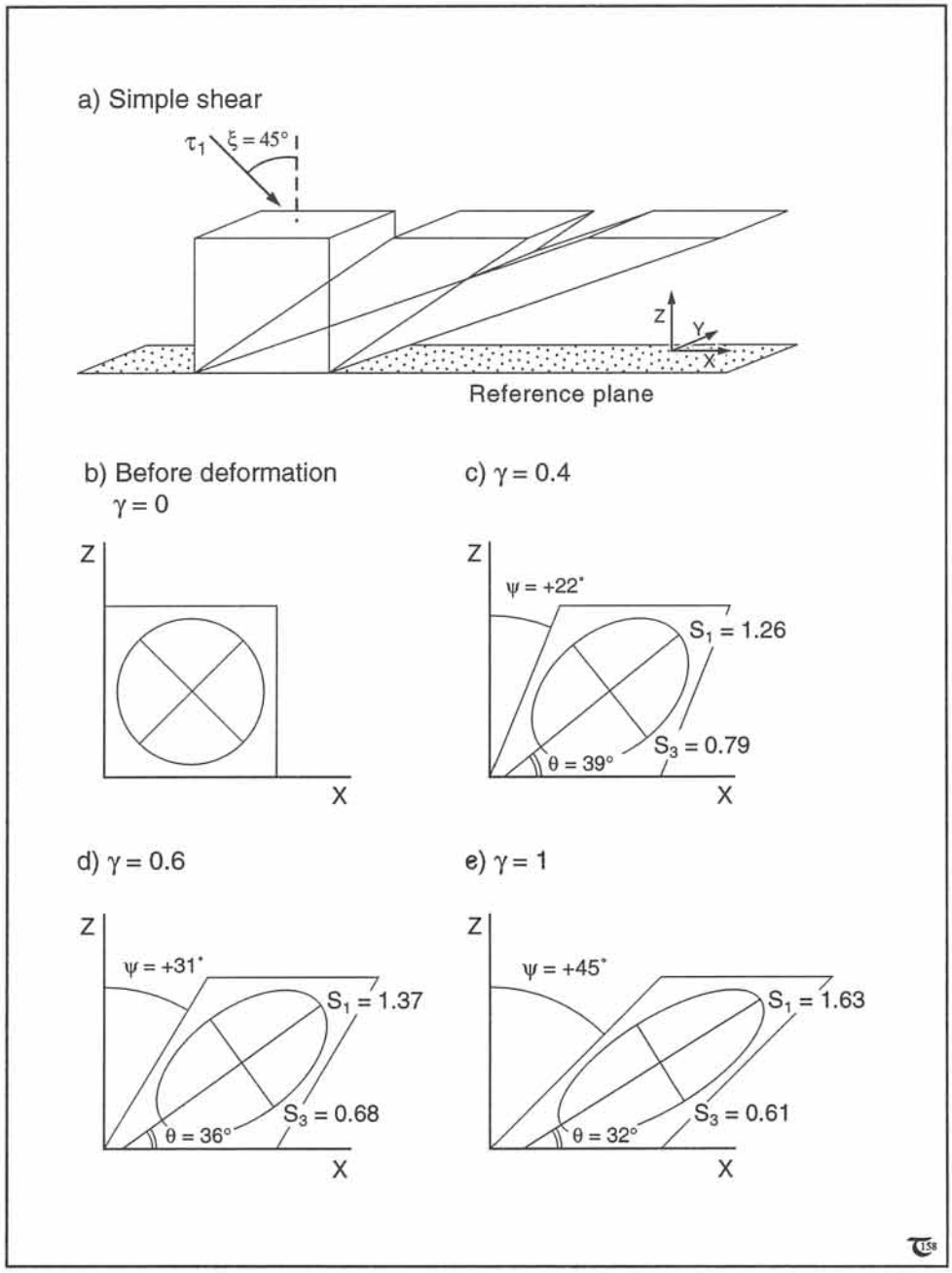

Figure 12-8: *a) to e) Simple shear deformation. This deformation is a special case of non-coaxial, plain strain, where the height of the sheared cube remains constant.*

direction of shear. The rotation angle or angular distortion, ψ, of the rotating vertical boundary provides a measure of distortional rotation, termed the *angular shear strain* or *engineering shear*, γ:

$$\gamma = \tan \psi \qquad (12\text{-}6)$$

The stretches, S_1 and S_3, change during progressive simple shear and relate to the angular shear strain, γ, by:

$$S_1 = [(1/2)[\gamma^2 + 2 + (\gamma^4 + 4\gamma^2)^{1/2}]]^{1/2} \qquad (12\text{-}7a)$$
$$S_3 = [(1/2)[\gamma^2 + 2 - (\gamma^4 + 4\gamma^2)^{1/2}]]^{1/2} \qquad (12\text{-}7b)$$

The changes of both S_1 and S_3 are graphed against γ in Figure 12-9a. The rotation angle, θ, between the major stretch axis, S_1, and the non-rotating base of the marker square (Fig. 12-8c) is another measure of distortional rotation:

$$\tan 2\theta = 2/\gamma \qquad (12\text{-}8)$$

Figure 12-9b graphs the relationship between θ and γ.

☐Exercise 12-5: a) What is the ultimate orientation of S_1 after an infinitely large simple shear? b) What is the height of a unit cube (cf., Fig. 12-8a) after infinitely large shear over its basal plane? c) Which material lines retain unit stretch throughout the deformation? Label those lines in Figure 12-8a.

☐Exercise 12-6: Consider an angular shear strain of magnitude 1 (unity). a) Calculate the values of ψ, S_1, S_3, and θ, using equations (12-6) to (12-8). b) Plot your values in Figures 12-9a & b. c) Check the outcome against the values in Figure 12-8e.

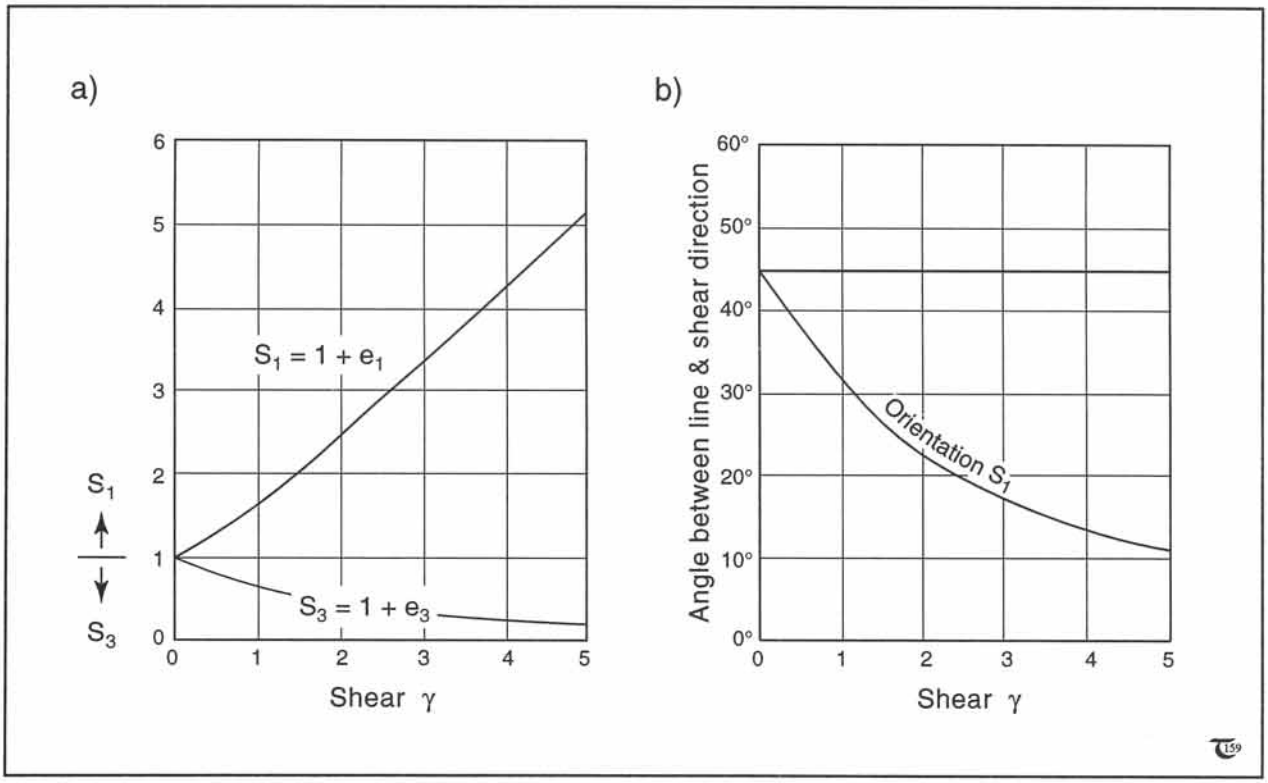

Figure 12-9: *a) Change of the principal stretches in simple shear deformation, as a function of angular shear strain. b) Change in orientation of the major stretch axis, as a function of angular shear strain.*

□Exercise 12-7: a) Plot ψ against θ, noting that at the onset of deformation $\psi=0°$ and $\theta=45°$, using three further pairs of (ψ,θ) from Figures 12-8c to e. b) Derive the mathematical relationship between ψ and θ, combining equations (12-6) and (12-8). c) Explain why θ is not equal to $[(90°-\psi)/2]$.

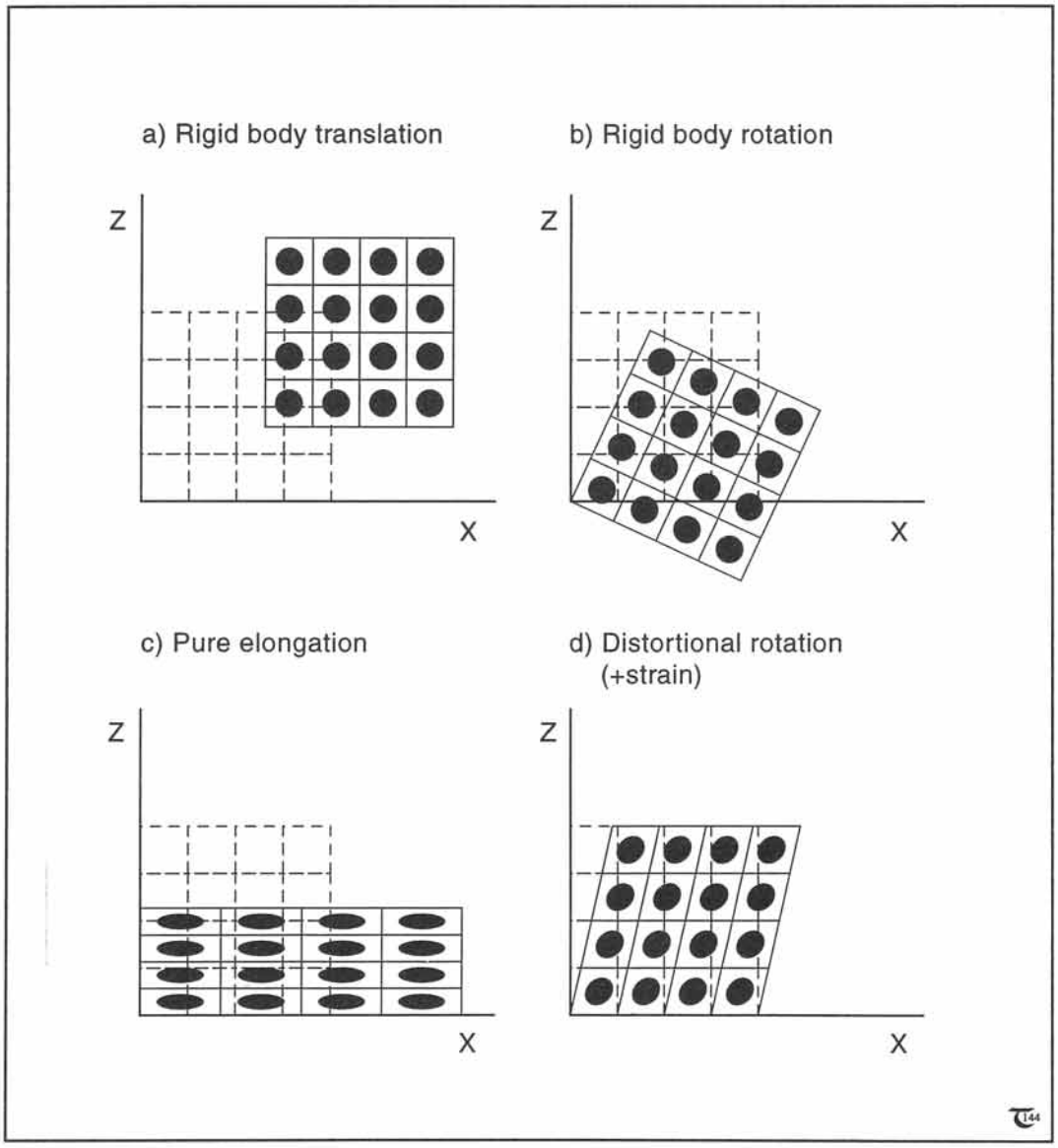

Figure 12-10: *a) to d) Four components of homogeneous and isochoric deformation.*

12-5 Components of deformation

Homogeneous deformation can comprise five components: volume change, rigid-body translation, rigid-body rotation, strain, and distortional rotation. Volume change has been considered separately in sections 11-2 and 15-6. The four components of isochoric deformation distinguished here may occur coevally in any rock volume, but they can be better understood if explained individually. A *rigid-body translation* spatially translates all material particles along parallel displacement paths (lines or curves) of equal length and involves neither a distortion of shape nor a change in the orientation of any marker grid (Fig. 12-10a). A *rigid-body rotation* rotates all material particles over the same angle with respect to a rotation center, and causes no distortion in shape, but does change the orientation of all material lines (Fig. 12-10b). *Pure elongation* causes changes in the shape of an undistorted strain circle, measuring changes or stretches of initial lengths (Fig. 12-10c). This component of deformation is irrotational in the sense that there is no rotation of the principal axes of strain during pure elongation alone. *Distortional rotation* is a component of simple shear deformation (Fig. 12-10d). It is a rotational strain and differs from a rigid-body rotation, which, if occurring alone, is not accompanied by a strain (Fig. 12-10b). The principal axes of strain rotate always during a distortional rotation.

Rigid-body translation and rigid-body rotation are commutative, in the sense that there is no difference in the final state, whether rotation occurs first and then the translation, or vice versa (Fig. 12-11a & b). However, the two components of deformation that may cause *distortion*, i.e., pure elongation and distortional rotation, cannot be superimposed commutatively. Figure 12-12a demonstrates a pure shear deformation, followed by a special distortional rotation, termed simple shear. Figure 12-12b superimposes these deformations in reverse order, and the final deformation state will be different from that seen in Figure 12-12a.

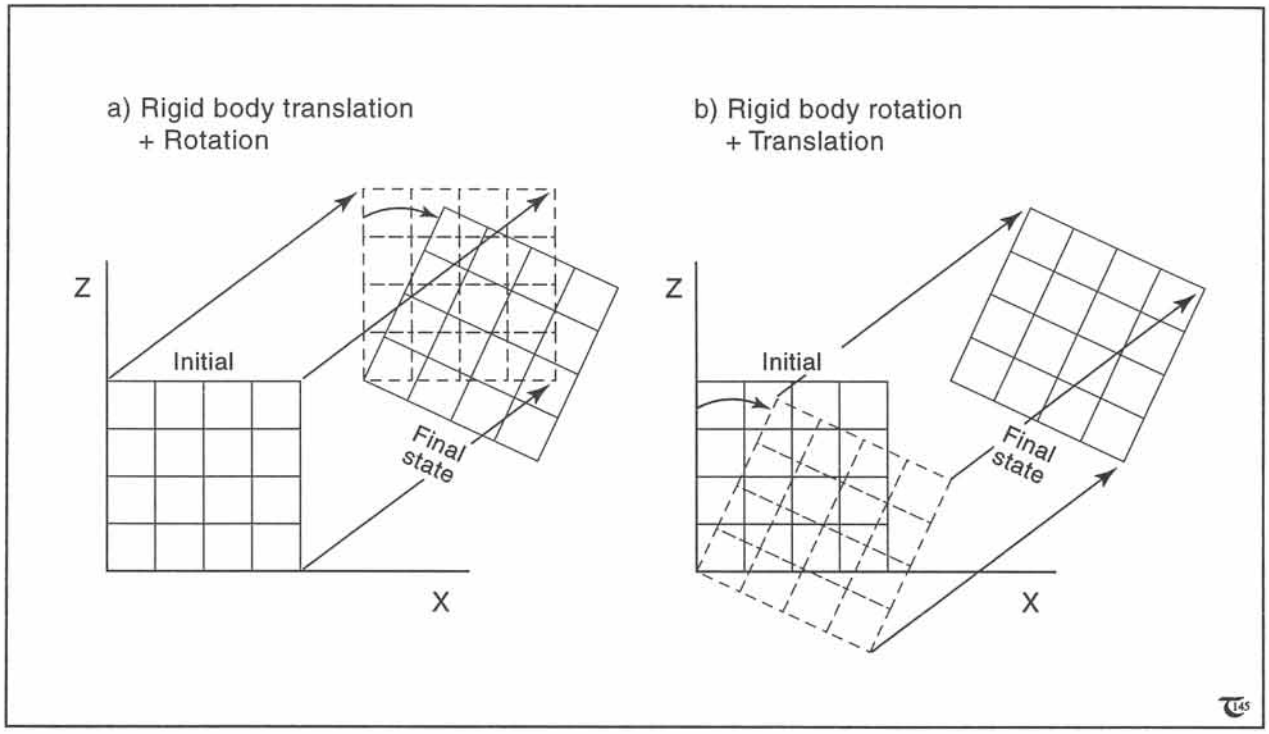

Figure 12-11: *a) & b) Rigid body rotation and translation are commutative deformation processes.*

Progressive deformation by pure shear and simple shear can be distinguished if the field relationships indicate that rock has deformed with one face adjacent to relatively undeformed wall rock. Figure 12-13a illustrates a unit volume of rock, deformed by a simple shear of 0.83 parallel to a perfectly lubricated stretching fault. Figure 12-13b achieves a similar finite deformation shape of the unit volume by 66% flattening by pure shear, assuming an appropriate initial orientation for the marker. The marked volume in the pure shear deformation (Fig. 12-13b) is indistinguishable from that in the simple shear deformation (Fig. 12-13a) after a 34° anti-clockwise rotation of the stretching fault. However, the strain ellipse in Figure 12-13b has deformed coaxially, and its stretching axis has remained parallel to the stretching fault at all times.

Strictly mathematically, it can be demonstrated indeed that a pure shear and a simple shear differ only by a rigid-body rotation and a rigid-body translation. This similarity has led to the common understanding among field geologists that it is impossible to determine whether a particular deformation pattern of plane strain has been formed by pure shear or simple shear. The mathematical similarities between a simple shaer (Fig. 12-13a) and a pure shear plus rigid-body rotation (Fig. 12-13b) is different from physical situations where ductile rock has flowed adjacent to physically rigid walls. In such situations, the stretching fault is a useful reference surface to distinguish the pure shear from a simple shear deformation. The stretching fault, also, is a useful reference boundary to determine the orientation of the major axis of the principal stress that must

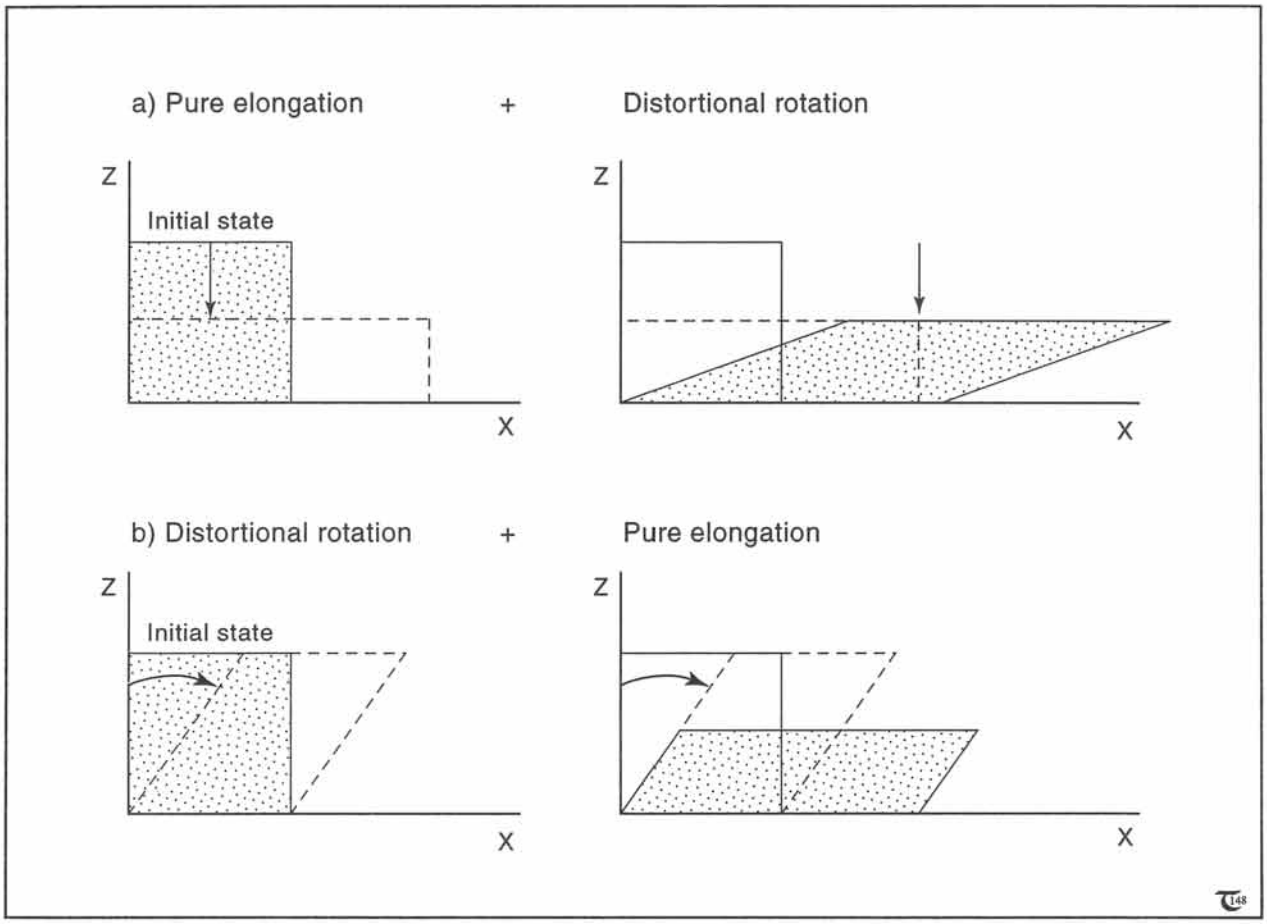

Figure 12-12: *a) & b) Pure elongation and distortional rotations; shown here are the special cases of pure shear and simple shear deformation. They are non-commutative deformation processes.*

☐**Exercise 12-8: Discuss why, in the absence of the fault reference surface, it is impossible to tell whether the *final* deformation, shown in Figure 12-13, was due to a pure or a simple shear.**

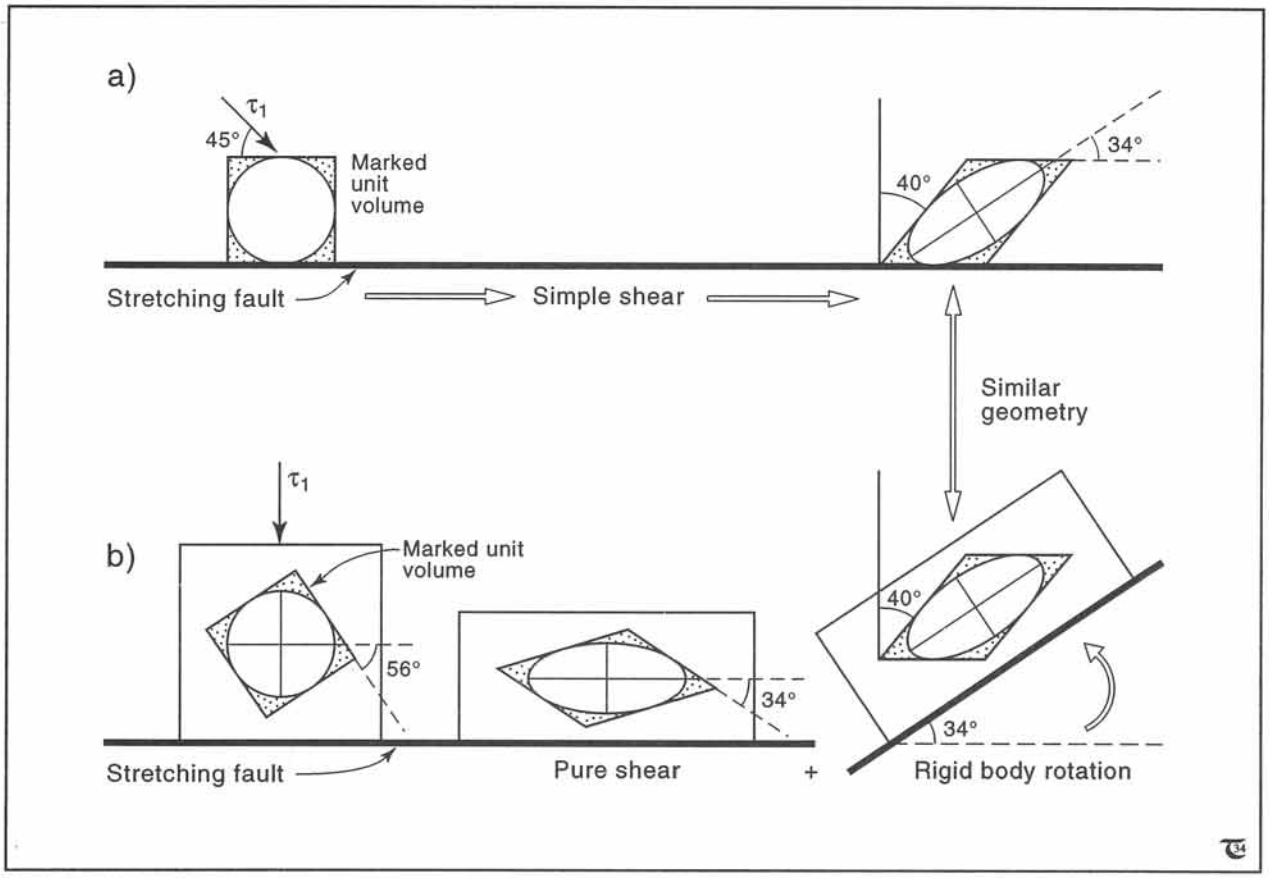

Figure 12-13: *a) & b) Similar deformation patterns may arise due to (a) simple shear, and (b) pure shear, followed by a rigid body rotation. However, the type of shear can still be told apart if a physical boundary, here a stretching fault, of the deforming rock volume is used as a reference surface for the distortion.*

have prevailed during the deformation. The principal deviatoric stress for a pure shear remains perpendicular to the stable boundary of the deforming rock volume, and is at 45° to that boundary for a simple shear deformation.

12-6 Deformation tensor

The changing shape of any material body in flow space can be expressed as a relative displacement of material points. Rigid-body translation and rotation can simply be removed from the analysis of deformation by choosing a coordinate system such that its origin coincides with material

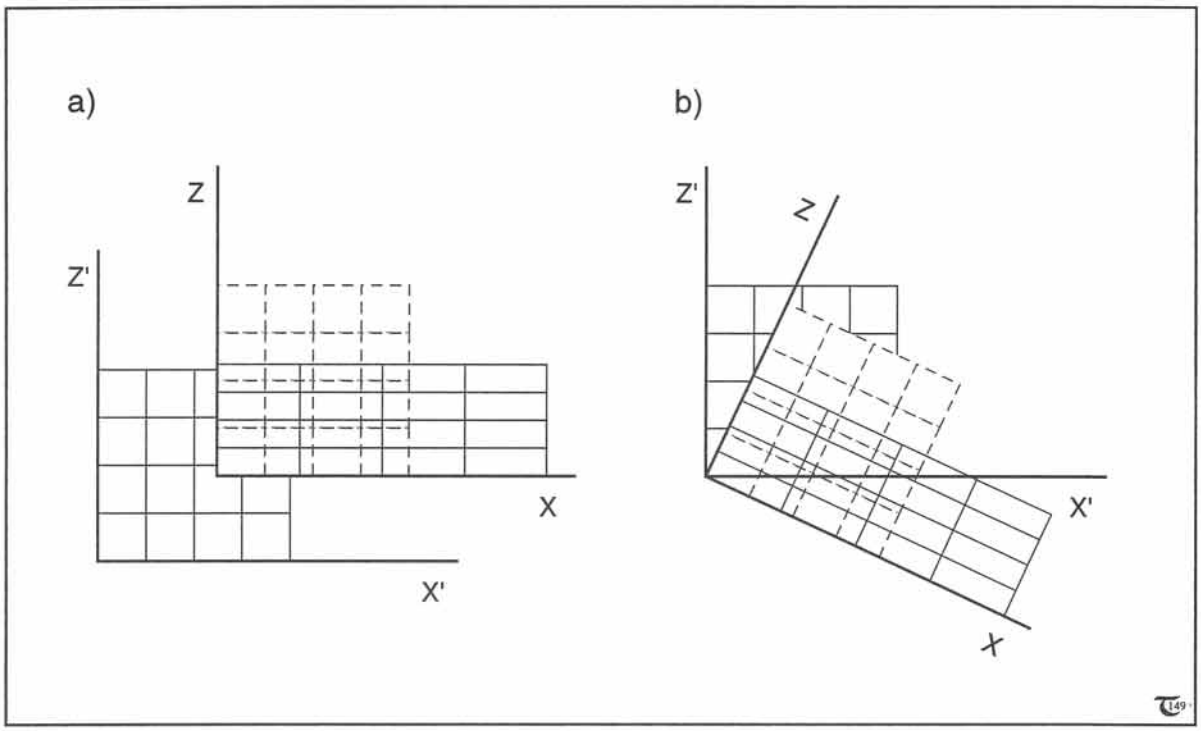

Figure 12-14: *a) & b) Rigid body translations (a) and rotations (b) can be distinguished in the description of distortions if the coordinate axes are kept parallel to the material boundaries of the undistorted rock volume.*

boundaries of the undistorted rock volume (Figs. 12-14a & b). The description of deformation is then reduced to its distortional components, i.e., irrotational strain and distortional rotation. *The challenging part of any description of deformation is to quantify the amount of distortional strain and distortional rotation experienced by a rock.*

If a *Cartesian description* is adopted, the position (x,y,z) of any point in the displaced state had coordinates (x_o,y_o,z_o) before its displacement. Any rigid-body translation is removed from the description by keeping, at least, one particle of the deforming body at the origin and translating the coordinate axes accordingly, if necessary. Figures 12-15a to c illustrate a pure shear, simple shear, and composite deformation, all within the XZ-plane. Normal (or pure shear) strain is defined as $d(x+u_1)/dx$ and (simple) shear strain as du_1/dz, so that finite deformation can be quantified if all the finite displacements u_i are known. The displacements, u_i, over a particular time interval, will vary in space as described by the displacement gradient tensor, **J** ($J_{ij}=\partial u_i/\partial x_j$):

$$u_i = J_{ij}x_j \qquad (12\text{-}9a)$$

The new position, x_i, of any particle, x_j, can then be described by the coordinate transformation:

$$x_i = (\delta_{kl}+J_{ij})x_j \qquad (12\text{-}9b)$$

with Kronecker's δ_{kl}. The matrix $(J_{ij}+\delta_{kl})$ is termed the deformation gradient or deformation tensor, F_{ij}.

Excluding rigid-body translations, the displacement, x_i, of original particles, x_j, in Eulerian space (XYZ) can now be described by the displacement equation:

$$x_i = F_{ij}x_j \qquad (12\text{-}10)$$

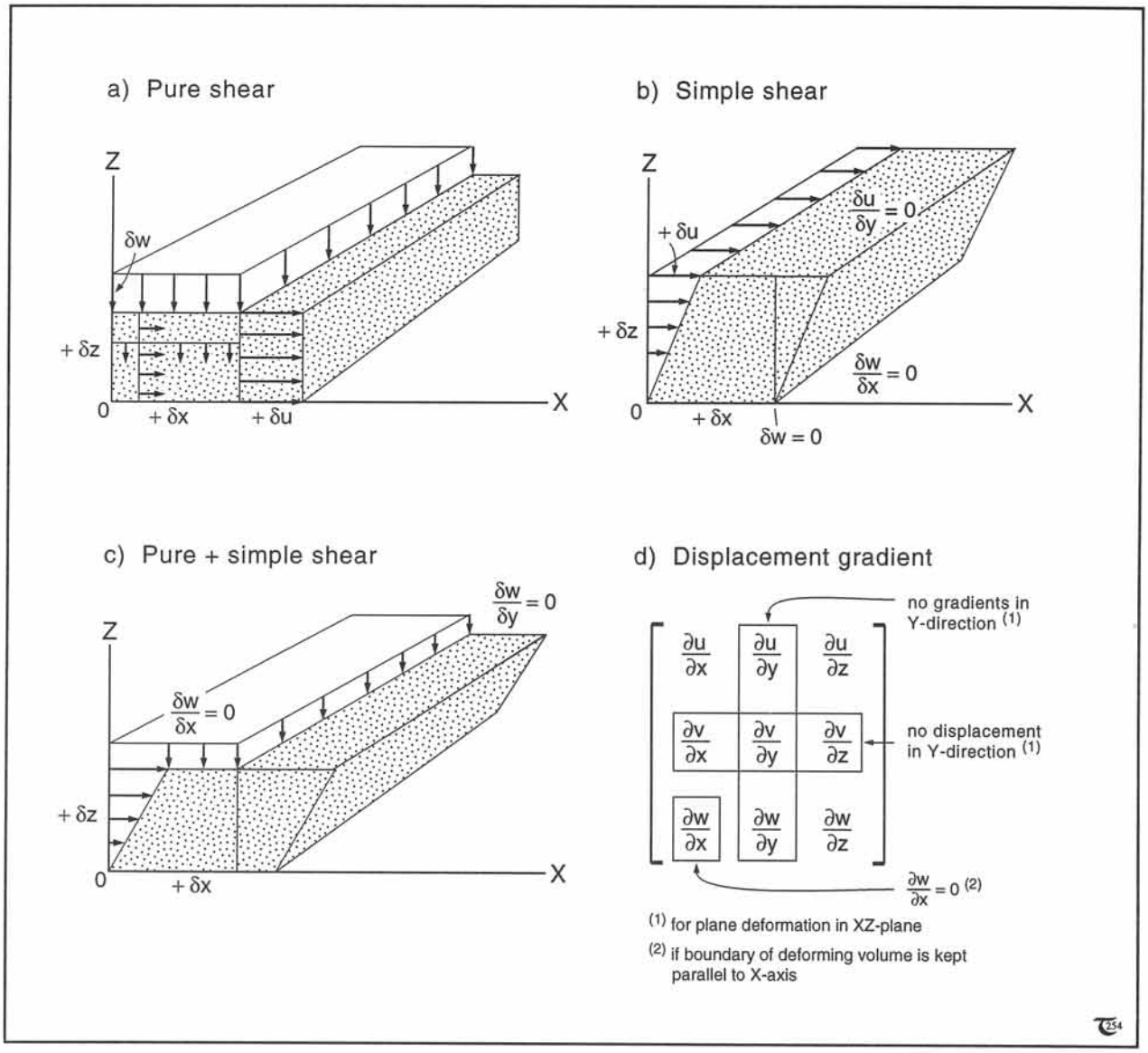

Figure 12-15: *a) to d) Examples of the various displacement gradients, featuring in the displacement gradient tensor, J_{ij} (featured in d).*

In the case of homogeneous deformation, the deformation tensor will be valid not only for infinitesimally small singularities, but even for finite volumes, provided rotation is taken into account.

It is worth noting that y_0 does not change in planar flows in the XZ plane, so that $y=y_0$ and $F_{22}=1$ in all such cases (Figs. 12-15a to c). For example, a unit simple shear has $F_{11}=F_{13}=F_{22}=F_{33}=1$, and all other tensor elements equal to zero. The corresponding particle coordinate transformation equations are: $x=x_0$, $y=y_0$, and $z=x_0+z_0$ [Fig. 12-15b, with angle $\tan^{-1}(du/dz)$]. A rigid-body translation has no displacement gradient, i.e., $\partial u_i/\partial x_j=0$, so that $F_{ij}=\delta_{ij}$. A 180° rigid-body rotation about the Y-axis in Cartesian XYZ-space has only three non-zero tensor elements, $F_{11}=F_{33}=-1$ and $F_{22}=1$ (Fig. 12-16).

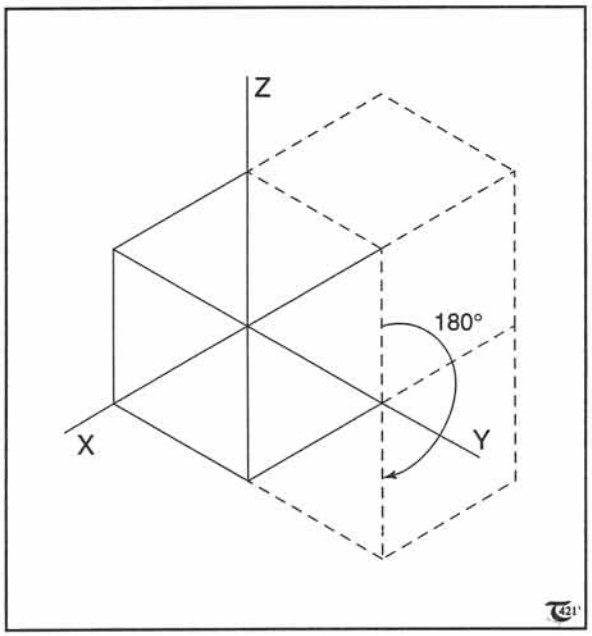

Figure 12-16: *Rigid body rotation about Y-axis can be represented by a symmetric deformation tensor with only three non-zero elements,* $F_{11}=F_{33}=-1$ *and* $F_{22}=1$.

☐Exercise 12-9: Give the deformation tensors for the deformations shown in Figures 12-17a & b.

☐Exercise 12-10: Figures 12-18a & b illustrate apparently non-commutative superpositions of a rigid body rotation and pure elongation. Study the sequence of events and explain how the finite elongation for both cases are, in fact, similar if coordinate axes and initial orientations of strain markers are chosen carefully.

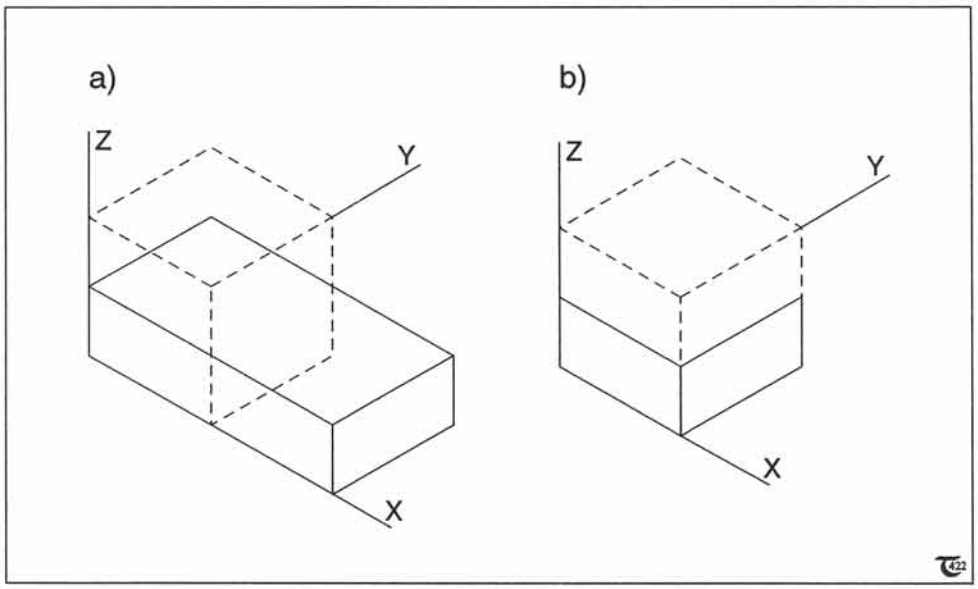

Figure 12-17: *a) & b) Examples of homogeneous deformations. See exercise 13-9.*

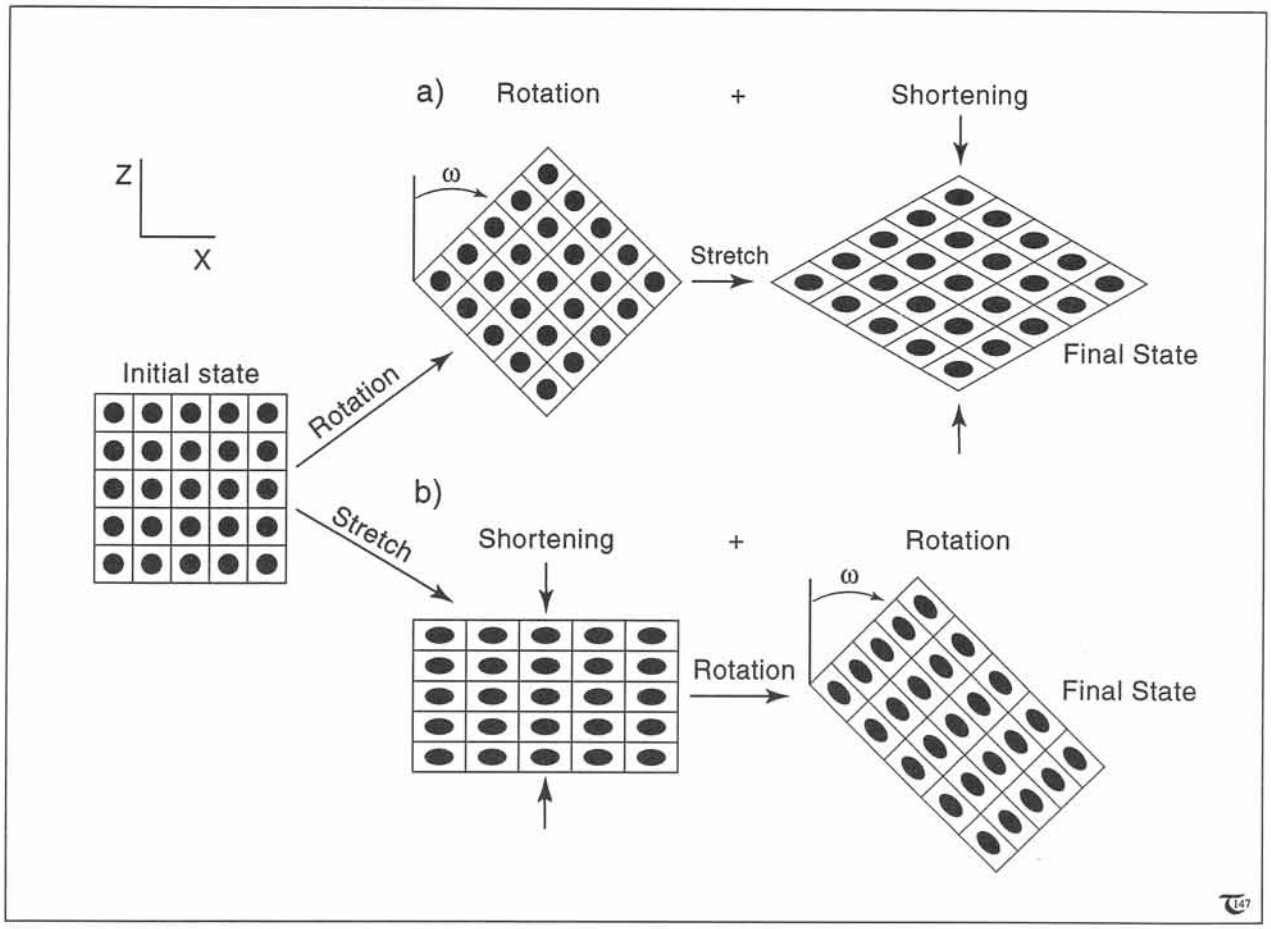

Figure 12-18: *a) & b) Superposition of rotation and pure elongation is not commutative in a strict sense. However, a smart choice of strain markers and coordinate axes will reveal both sequences result in identical finite elongations, differing in orientation only by a rigid body rotation. See exercise 12-10.*

12-7 Length and orientation of principal stretches

Figures 12-19a and b explain how the matrix elements, F_{11}, F_{13}, and F_{33}, are physically expressed as the normalized dimensions of a cubic (unit) volume, deforming in two-dimensional or planar flow along a stable detachment horizon or reference plane. The angle, β, between the detachment surface and any surface rotated normal to the detachment surface is (Fig. 12-19b):

$$\beta=\tan^{-1}(F_{33}/F_{13}) \qquad (12\text{-}11)$$

The principal stretches, S_1 and S_3, of the principal ellipse section of a strain ellipsoid for a plane deformation (Fig. 12-16c) can be determined from the deformation tensor elements, F_{11}, F_{13}, F_{31}, and F_{33}, as follows:

$$S_1=[0.5(K+[K^2-4(F_{11}F_{33}-F_{13}F_{31})^2]^{1/2})]^{1/2} \qquad (12\text{-}12a)$$
$$S_3=[0.5(K-[K^2-4(F_{11}F_{33}-F_{13}F_{31})^2]^{1/2})]^{1/2} \qquad (12\text{-}12b)$$

with $K=F_{11}^2+F_{13}^2+F_{31}^2+F_{33}^2$. One can see that a rigid-body translation, which has tensor elements $F_{11}=F_{22}=F_{33}=1$ and $F_{13}=F_{31}=0$, yields a unit circle with $S_1=S_3=1$. The angle, θ_S, between the finite strain ellipsoid's major axis and the X-axis is:

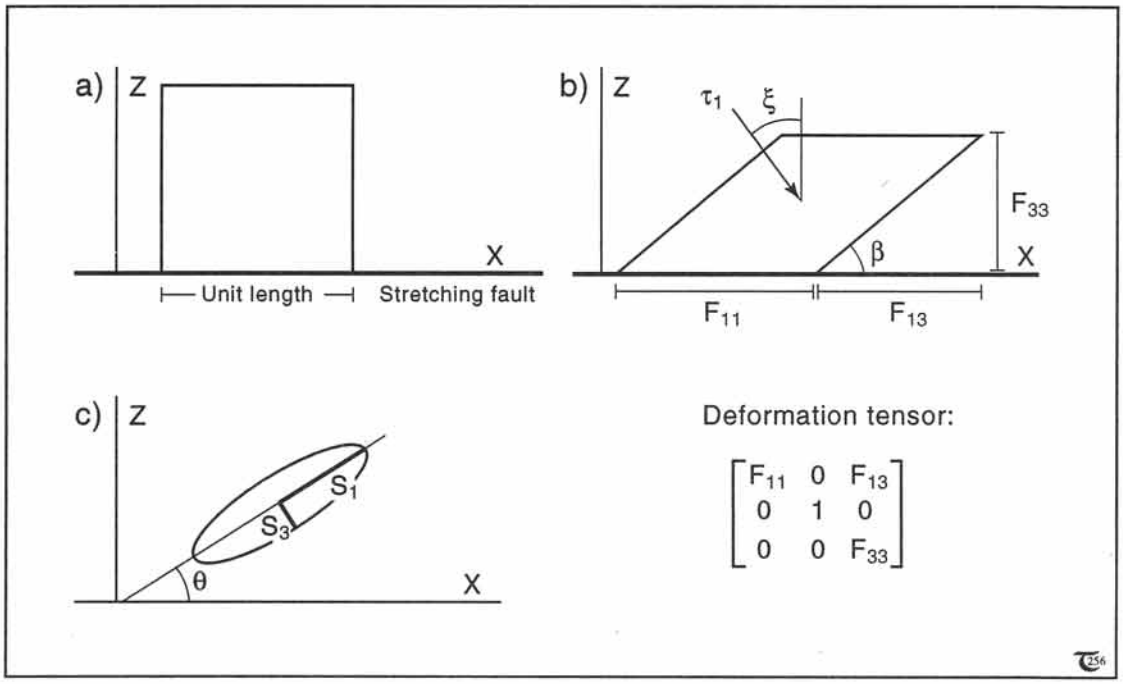
a)
Z
X
Unit length
Stretching fault
b)
Z
τ_1
ξ
F_{33}
β
X
F_{11}
F_{13}
c)
Z
S_1
S_3
θ
X
Deformation tensor:
$\begin{bmatrix} F_{11} & 0 & F_{13} \\ 0 & 1 & 0 \\ 0 & 0 & F_{33} \end{bmatrix}$

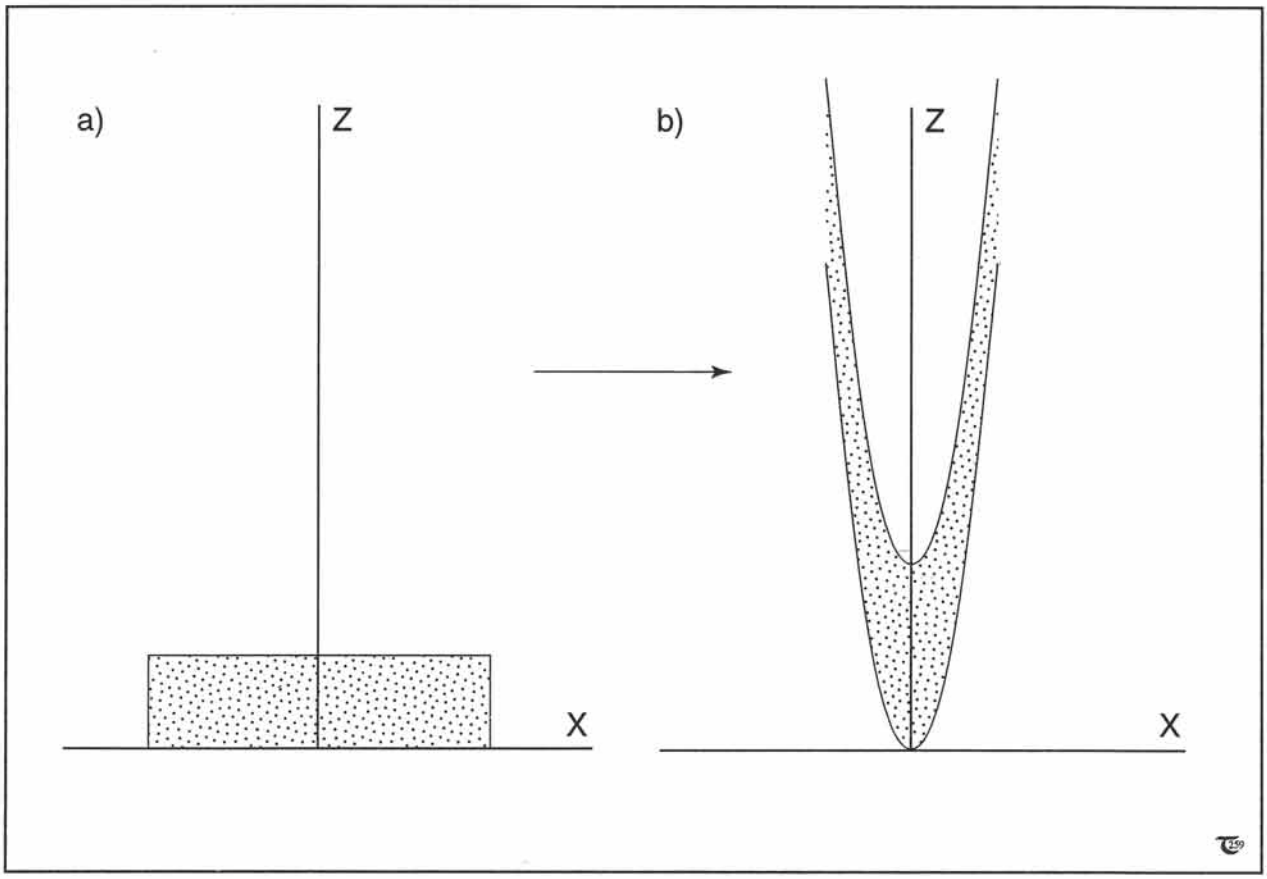
a)
Z
X
b)
Z
X

Figure 12-19: a) to c) Deformation matrix elements can be physically represented by the dimensions of a parallelopiped (b), which corresponds to a unit square in an undeformed state (a). (c) The finite strain ellipse stretches (S_1 and S_3) and orientation (θ) can all be calculated from the deformation tensor, according to equations (12-12a & b) and (12-13).

$$\theta_S = 0.5 \operatorname{atan}[(2F_{11}F_{31}-2F_{13}F_{33})/(F_{11}^2+F_{13}^2-F_{31}^2-F_{33}^2)] \quad (12\text{-}13)$$

Substitution of the F_{ij} values for a unit simple shear yields $\theta_S = 31.7°$.

☐Exercise 12-11: Give the stretches of the strain ellipsoids for the deformations of Figures 12-17a & b.

☐Exercise 12-12: The deformation tensor for the fold structure in Figure 12-20 is given by $F_{11}=0.5$, $F_{13}=0$, $F_{22}=1$, $F_{33}=2$, and $F_{31}=x_0$, with all other components equal to zero. Calculate the principal stretches and the orientation of the finite strain ellipsoids for infinitesimally small particles within the folded layer at $x_0=0$, 2, 4, 8, and 10. Make a blow-up figure of one fold limb, and draw the strain ellipse orientation and ellipticity to scale for each point calculated.

Figure 12-20: a) & b) Initial state of a layer before and after deformation, resulting in quasi-similar fold-shape and 50% horizontal shortening. This deformation is fully described by the following transformations: $x=0.5x_0$ and $z=x_0^2+2z_0$. See exercise 12-12.

12-8 Decomposition of deformation tensor

The variable part of the deformation tensor, F_{ij} ($=\delta_{kl}+\partial u_i/\partial x_j$), is the displacement-gradient tensor, **J**. For infinitesimal deformations, the displacement-gradient tensor can be separated into the sum of a symmetric matrix, E_{ij}, and skew-symmetric matrix, Ω_{ij}:

$$J_{ij} = E_{ij} + \Omega_{ij} \quad (12\text{-}14)$$

The symmetric matrix describes the strain component of the deformation and is, therefore, called the strain matrix:

$$E_{ij} = (1/2)[(\partial u_i/\partial x_j)+(\partial u_j/\partial x_i)] = \begin{bmatrix} e_{11} & \gamma_{12}/2 & \gamma_{13}/2 \\ \gamma_{21}/2 & e_{22} & \gamma_{23}/2 \\ \gamma_{31}/2 & \gamma_{32}/2 & e_{33} \end{bmatrix} \quad (12\text{-}15a)$$

It is worth noting that the geoscience literature sometimes confusingly uses the term *strain matrix* for what is, in effect, the *displacement-gradient matrix*, and vice versa. The rotation component of any deformation can be expressed by the skew-symmetric rotation matrix:

$$\Omega_{ij} = (1/2)[(\partial u_i/\partial x_j)-(\partial u_j/\partial x_i)] = \begin{bmatrix} 0 & \omega_3/2 & -\omega_2/2 \\ -\omega_3/2 & 0 & \omega_1/2 \\ \omega_2/2 & -\omega_1/2 & 0 \end{bmatrix} \quad (12\text{-}15b)$$

with principal rotations, ω_k.

The above decomposition of the deformation matrix cannot be applied to finite deformations, as non-linear terms need to be taken into account for large deformations. However, finite deformation patterns and the associated finite strains and rotations may be determined by stepwise superimposition of small increments of strain and rotation. The finite strains, displayed in Figure 12-21, were constructed from the particle movement paths after integration of the rate of displacement equations, which accounts for the non-linearity of

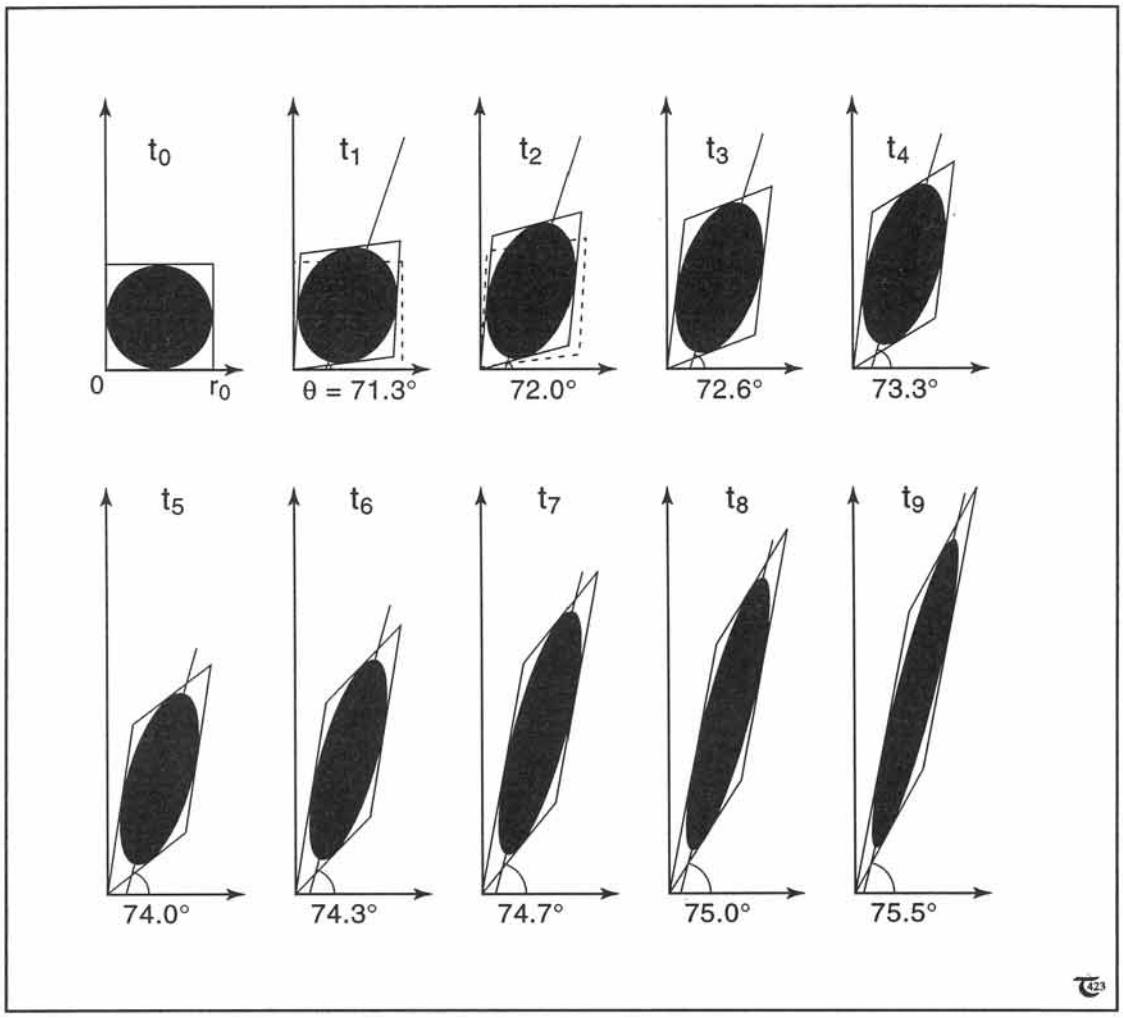

Figure 12-21: *Sequence of progressive deformation by plane strain corresponding to the deformation tensor elements of Table 12-2. See exercise 12-13.*

	F_{11}	F_{13}	F_{31}	F_{33}	S_1	S_3	θ
Stage 0	1	0	0	1	1	1	-
Stage 1	0.9136	0.0500	0.1000	1.1000	1.13	0.89	71.29
Stage 2	0.8397	0.1007	0.2014	1.2150	1.27	0.79	71.99
Stage 3	0.7772	0.1527	0.3055	1.3466	1.43	0.70	72.64
Stage 4	0.7253	0.2068	0.4138	1.4985	1.61	0.62	73.25
Stage 5	0.6833	0.2638	0.5277	1.6668	1.81	0.55	73.79
Stage 6	0.6506	0.3243	0.6488	1.8599	2.04	0.49	74.27
Stage 7	0.6268	0.3893	0.7787	2.0783	2.30	0.44	74.68
Stage 8	0.6116	0.4596	0.9193	2.3251	2.59	0.39	75.04
Stage 9	0.6047	0.5361	1.0724	2.6036	2.91	0.34	75.51

Table 12-2: *Numerical values of non-zero deformation tensor elements (F_{ij}), stretches (S_1 and S_3), and orientation (θ) of the finite strain ellipses for the nine deformation stages, illustrated in Figure 12-21. See exercise 12-13.*

large deformations. The deformation tensor elements for each stage in the deformation are given in Table 12-2, together with the principal stretches, S_1 and S_3, and the orientation, θ, of the finite strain ellipse.

If a principal strain-rate of an irrotational deformation is known, then the stretch, S_1, at each instant of time, t, elapsed since the onset of the deformation is given by the following equation:

$$S_1 = \exp(\dot{e}_1 t) \qquad (12\text{-}16)$$

For details, see exercise 13-6 in chapter 13.

☐Exercise 12-13: Check some of the values in Table 12-2 for the stretches and orientation of the finite strain ellipse, using equations (12-12a & b) and (12-13).

References

Articles

The following articles provide useful complementary reading to the topics discussed in this chapter:

Hsu, T.C. (1966, *Journal of Strain Analysis*, volume 1, pages 216 to 222). The characteristics of coaxial and non-coaxial strain paths.

McKenzie, D.P. (1979, *Geophysical Journal of the Royal Astronomical Society*, volume 58, pages 689 to 715). Finite deformation during fluid flow.

McKenzie, D.P. and Jackson, J. (1983, *Earth and Planetary Science Letters*, volume 65, pages 182 to 202). The relationship between strain rates, crustal thickening, paleomagnetism, finite strain, and fault movements within a deforming zone.

Pfiffner, O.A. and Ramsay, J.G. (1982, *Journal of Geophysical Research*, volume 87, pages 311 to 321). Constraints on geological strain-rates; arguments from finite strain states of naturally deformed rocks.

Ramberg, H. (1975, *Tectonophysics*, volume 28, pages 1 to 37). Particle paths, displacement and progressive strain applicable to rocks. See, also, correction in Ramberg (1986, *Tectonophysics*, volume 121, page 355).

Weijermars, R. (1988, *American Journal of Physics*, volume 56, pages 534 to 540). Progressive fluid deformation in low Reynolds number flow past a falling cylinder.

Weijermars, R. (1989, *Earth and Planetary Science Letters*, volume 91, pages 367 to 373). Experimental pictures of deformation patterns in a possible model of the Earth's interior.